Defining tissue specific gene sets using Bayesian unsupervised clustering

GEN80436

Stephen Coleman
940309160050

supervised by
Bas Zwaan
Laboratory of Genetics, Wageningen University
and
Chris Wallace
Department of Medicine, Cambridge University

Abstract

A priori defined gene sets are key to gene set enrichment analysis [20] a powerful tool in genetic analysis. Gene sets are constructed through linking genes by some common feature. This can be a function, the location of the gene product, the participation of the product in some metabolic or signalling pathway, the protein structure, the presence of transcription-factor-binding sites or other regulatory elements, the participation in multiprotein complexes, or any one of several other definitions [21][20][7][1]. However, all of these criteria are tissue agnostic. We propose to produce tissue specific gene sets by applying multiple dataset integration [8] (a Bayesian unsupervised clustering method) to the gene expression data from the CEDAR cohort [23], a dataset of 9 tissue / cell types.

A thesis presented for the degree of
Master's in Bioinformatics

Wageningen University

1 Introduction

This project, which consists of applying a Bayesian unsupervised clustering method across multiple datasets to define tissue specific gene sets, is interesting on a number of fronts. It provides a chance to learn relevant, topical biology in understanding gene sets, the role context plays in gene expression and to learn the basics of immunology. From an informatics / statistics perspective, Bayesian inference, unsupervised clustering and the use of multiple datasets are all interesting. These are relevant skills to both industry and research that I wish to develop.

Beyond developing new skills, this project also offers the opportunity to be involved in relevant research. Gene sets are commonly used in genetic analyses, thus if we can produce sets that are informed by the context of interest, it could be relevant to many researchers. Hopefully by producing more informative gene sets we can help narrow the gap between biology and disease.

2 Theory

2.1 Clustering

Given data $X = (x_1, \ldots, x_n)$, we define a *clustering* or partition of the data by:

$$
\begin{align}
Y &= \{Y_1, \ldots, Y_K\} \tag{1}\\
Y_k &= \{x_{1_k}, \ldots, x_{n_k}\} \tag{2}\\
Y_i \cap Y_j &= \varnothing \ \forall \ i, j \in \{1, K\}, i \neq j \tag{3}\\
n_k &\geq 1 \ \forall \ k \in \{1, K\} \tag{4}\\
\sum_{k=1}^{K} n_k &= n \tag{5}
\end{align}
$$

In short we have K nonempty disjoint sets of data, each of which is referred to as a *cluster*, the set of which form a *clustering*. We define a *label* $c = (c_1, \ldots, c_n)$ as denoting the membership of each point. A label $c_i = k$ states that point x_i is assigned to cluster Y_k.

2.2 Mixture models

Given some data $X = (x_1, \ldots, x_n)$, we assume a number of unobserved processes generate the data, and membership to a process for individual i is represented using the latent variable c_i. It is assumed that each of the K processes can be modelled by a parametric distribution, $f(\cdot)$ with associated parameters θ and that the full model density is then the weighted sum of these probability density functions where the

weights are the component proportions, π_k:

$$p(x_i) = \sum_{k=1}^{K} \pi_k f(x_i|\theta_k) \tag{6}$$

2.3 Bayesian inference

We carry out Bayesian inference of this model using Markov chain Monte Carlo methods. We sample first the component parameters, θ_k, and associated weights, π_k, from the associated distributions and then sample component membership.
Basically:

1. For each of K clusters sample θ_k and π_k from the associated distributions based on current memberships, c_i; and

2. For each of n individuals sample c_i based on the new θ_k and π_k.

For the mixture model we update the parameters after we allocate each observation to a cluster. For a given cluster with associated data X and parameter θ, we sample θ using Bayes' theorem from the distribution:

$$p(\theta|X) = \frac{p(X|\theta)p(\theta)}{\int_\Theta p(X|\theta')p(\theta')d\theta'} \tag{7}$$

Here Θ is the entire sample space for θ.

- We refer to $p(\theta|X)$ as the *posterior* distribution of θ as it is the distribution associated with θ *after* observing X.

- $p(\theta)$ is the *prior* distribution of θ and captures our beliefs about θ before we observe X.

- $p(X|\theta)$ is the *likelihood* of X given θ, the probability of data X being generated given our model is true. It is the criterion we focus on in our model if we would use a frequentist approach to the inference; maximising this quantity in our model generates the curve that best describes the observed data.

- $\int_\Theta p(X|\theta')p(\theta')d\theta'$ is the *normalising constant*. This quantity is also referred to as the *evidence* [11] or *marginal likelihood* and is normally represented by Z. It is referred to as the marginal likelihood as we marginalise the parameter θ by integrating over its entire sample space.

In terms of sampling, the prior is very useful as a clever choice of prior can ensure that the posterior is always solvable, that we do not encounter singularities in our distribution.

2.4 Multiple dataset integration

Consider the case when we have observed paired datasets $X_1 = (x_{1,1}, \ldots, x_{n,1})$, $X_2 = (x_{1,2}, \ldots, x_{n,2})$, where observations in the ith row of each dataset represent information about the same individual. We would like to cluster individuals using information common to both datasets. One could concatenate the datasets, adding additional covariates for each individual. However, if the two datasets have different clustering structures this would reduce the signal of both clusterings and probably have one dominate. If the two datasets have the same structure but different signal-to-noise ratios this would reduce the signal in the final clustering. In both these cases independent models on each dataset would be preferable. Kirk et al. [8] suggest a method to carry out clustering on both datasets where common information is used but two individual clusterings are outputted. This method is driven by the allocation prior:

$$p(c_{i1}, c_{i2}|\phi) \propto \pi_{i1}\pi_{i2}(1 + \phi\mathbb{I}(c_{i1} = c_{i2})) \tag{8}$$

Here $\phi \in \mathbb{R}_+$ controls the strength of association between datasets. (8) states that the probability of allocating individual i to component $c_{i,1}$ in dataset 1 and to component $c_{i,2}$ in dataset 2 is proportional to the proportion of these components within each dataset and up-weighted by ϕ if the individual has the same labelling in each dataset. Thus as ϕ grows the correlation between the clusterings grow and we are more likely to see the same clustering emerge from each dataset. Conversely if $\phi = 0$ we have independent mixture models.

The generalised case for L datasets, $X_1 = (x_{1,1}, \ldots, x_{n,1}), \ldots, X_L = (x_{1,l}, \ldots, x_{n,l})$ for any $L \in \mathbb{N}$ is simply a matter of combinatorics. In this case, (8) extends to:

$$p(c_{i1}, \ldots, c_{iL}|\boldsymbol{\phi}) \propto \left[\prod_{l_1=1}^{L} \pi_{c_{il_1}l_1}\right] \left[\prod_{l_2=1}^{L-1} \prod_{l_3=l_2+1}^{L} \left(1 + \phi_{l_2l_3}\mathbb{1}(c_{il_2} = c_{il_3})\right)\right] \tag{9}$$

Here $\boldsymbol{\phi}$ is the $\binom{L}{2}$-vector of all ϕ_{ij} where ϕ_{12} is the variable ϕ in (8).

Thus MDI is an extension of mixture models to multiple datasets where correlated clustering structure is used to "upweigh" similar clusters across datasets. MDI has been applied to precision medicine, specifically glioblastoma sub-typing [19], in the past showing its potential as a tool.

2.5 Rand index

A popular metric for comparing the similarity of two clusterings of the data is the *Rand index* [18]. If one assumes that all points are of equal importance in determining clusterings, then in combination with the discrete nature of clusters and the fact that a cluster is defined as much by what it does not contain as that which it does, Rand [18] proposes a metric to measure similarity between clusterings. Between

3

$Y \diagdown{}^{Y'}$	Y'_1	Y'_2	$\cdots$	$Y'_{K'}$	Sums
Y_1	n_{11}	n_{12}	$\cdots$	$n_{1K'}$	$n_{1\cdot}$
Y_2	n_{21}	n_{22}	$\cdots$	$n_{2K'}$	$n_{2\cdot}$
$\vdots$	$\vdots$	$\vdots$	$\ddots$	$\vdots$	$\vdots$
Y_K	n_{K1}	n_{K2}	$\cdots$	$n_{KK'}$	$n_{K\cdot}$
Sums	$n_{\cdot 1}$	$n_{\cdot 2}$	$\cdots$	$n_{\cdot K'}$	$n_{\cdot\cdot} = n$

Table 1: Contingency table used by Rand [18] to calculate a measure of similarity between clusterings Y and Y'.

clusterings Y and Y' for any two points x_i and x_j there can exist one of a number of scenarios regarding their labeling. Let γ_{ij} be a measure between the two points x_i and x_j. For the two points, they can have:

1. the same label in both clusterings ($c_i = c_j \wedge c'_i = c'_j$) ($\gamma_{ij} = 1$);

2. different labels in both ($c_i \neq c_j \wedge c'_i \neq c'_j$) ($\gamma_{ij} = 1$); or

3. the same label in one but not in the other ($c_i \neq c_j \wedge c'_i = c'_j \vee c_i = c_j \wedge c'_i \neq c'_j$) ($\gamma_{ij} = 0$).

Thus Rand [18] propose counting the number of times any two points have one of 1 or 2 from list 2.5 and finding the proportion of these compared to the number of all possible point combinations. More formally, this is:

$$A \binom{n}{2}^{-1} = \frac{1}{\binom{n}{2}} \sum_{i=1}^{n-1} \sum_{j=i+1}^{n} \gamma_{ij} \tag{10}$$

This can be envisioned as a $K \times K'$ contingency table of the count of overlapping points, as shown in table 1. Table 1 uses the following notation:

- n_{ij} is the number of points that have membership in Y_i in clustering Y and Y'_j in clustering Y';

- $n_{\cdot j}$ is the number of points in cluster Y'_j in clustering Y';

- $n_{i\cdot}$ is the number of points in cluster Y_i in clustering Y; and

- $n_{\cdot\cdot} = n$ is the number of points in clusterings Y and Y'.

One can restate equation 10 in terms of the notation from table 1 citeBrennanLight:

$$A = \binom{n}{2} + \sum_{i=1}^{K} \sum_{j=1}^{K'} n_{ij}^2 - \frac{1}{2} \left(\sum_{i=1}^{K} n_{i\cdot}^2 + \sum_{j=1}^{K'} n_{\cdot j}^2 \right) \tag{11}$$

$$= \binom{n}{2} + 2 \sum_{i=1}^{K} \sum_{j=1}^{K'} \binom{n_{ij}}{2} - \left[\sum_{i=1}^{K} \binom{n_{i\cdot}}{2} + \sum_{j=1}^{K'} \binom{n_{\cdot j}}{2} \right] \tag{12}$$

4

Hubert and Arabie [5] extend the Rand index to account for chance. They include a null hypothesis and assume that there is a probability of some points having a γ value of 1 by chance. Consider the scenario where a point x_i has the same label as another point x_j under clustering Y. For another clustering Y', there a non-zero is a probability $c'_i = c'_j$ purely by chance and does not represent a similarity between Y and Y'. If one generates two clusterings Y and Y' by sampling from the integers in the closed interval $[1, K]$ (i.e. by sampling from discrete unfirom distribution $\mathcal{U}\{1, K\}$), then the contingency table generated is constructed from the generalised hyper-geometric distribution [5]. It can be shown that the expected number of points with common membership in both clusters is non-zero. Specifically:

$$\mathbb{E}\left(\sum_{i=1}^{K}\sum_{j=1}^{K}\binom{n_{ij}}{2}\right) = \frac{\sum_{i=1}^{K}\binom{n_{i\cdot}}{2}\sum_{j=1}^{K}\binom{n_{\cdot j}}{2}}{\binom{n}{2}} \tag{13}$$

This is the product of the number of distinct pairs that can be formed from rows and the number of distinct pairs that can be constructed from columns, divided by the total number of pairs.

For a particular cell of the contingency table, the expected number of entries of the type described in point 1, is the product of number of pairs in its row and in its column divided by the total number of possible pairs:

$$\mathbb{E}\left(\binom{n_{ij}}{2}\right) = \frac{\binom{n_{i\cdot}}{2}\binom{n_{\cdot j}}{2}}{\binom{n}{2}} \tag{14}$$

One can see that as each component of equation 11 is some transformation of $\sum_{i,j}\binom{n_{ij}}{2}$, one can directly state the expected value of the Rand index by combining equations 11 and 14:

$$\mathbb{E}\left(A\binom{n}{2}^{-1}\right) = 1 + 2\sum_{i=1}^{K}\binom{n_{i\cdot}}{2}\sum_{j=1}^{K'}\binom{n_{\cdot j}}{2}\binom{n}{2}^{-2} - \left[\sum_{i=1}^{K}\binom{n_{i\cdot}}{2} + \sum_{j=1}^{K'}\binom{n_{\cdot j}}{2}\right]\binom{n}{2}^{-1} \tag{15}$$

Defining an index corrected for chance as:

$$\text{Corrected index} = \frac{\text{Index} - \text{Expected index}}{\text{Maximum index} - \text{Expected index}} \tag{16}$$

Assuming a maximum value of 1 for the Rand index then gives a corrected Rand index:

$$\frac{\sum_{i=1}^{K}\sum_{j=1}^{K'}\binom{n_{ij}}{2} - \sum_{i=1}^{K}\binom{n_{i\cdot}}{2}\sum_{j=1}^{K'}\binom{n_{\cdot j}}{2}\binom{n}{2}^{-1}}{\frac{1}{2}\left[\sum_{i=1}^{K}\binom{n_{i\cdot}}{2} + \sum_{j=1}^{K'}\binom{n_{\cdot j}}{2}\right] - \sum_{i=1}^{K}\binom{n_{i\cdot}}{2}\sum_{j=1}^{K'}\binom{n_{\cdot j}}{2}\binom{n}{2}^{-1}} \tag{17}$$

We define this quantity described in equation 17 as the *adjusted Rand index* and we use it as our measure of choice for similarity between clusterings.

We describe an explicit example motivating the adjusted Rand index in section 2.5.1.

Y \ Y'	Y'_1	Y'_2	Y'_3	Sums
Y_1	$\frac{n}{2}$	$\frac{n}{16}$	$\frac{n}{16}$	$\frac{10n}{16}$
Y_2	$\frac{n}{16}$	$\frac{n}{16}$	$\frac{n}{16}$	$\frac{3n}{16}$
Y_3	$\frac{n}{16}$	$\frac{n}{16}$	$\frac{n}{16}$	$\frac{3n}{16}$
Sums	$\frac{10n}{16}$	$\frac{3n}{16}$	$\frac{3n}{16}$	$\frac{16n}{16} = n$

Table 2: Contingency table for the non-random clustering described in section **??**.

2.5.1 Motivating example: adjusted Rand index

Consider the case of n labels Y and Y' generated from $\mathcal{U}\{1,3\}$ where n is some arbitrarily large number. Then as n tends to infinity we can expect that our contingency table has entries of $\frac{n}{9}$ in each cell. If one calculates the Rand index on these random partitions where any similarity is purely by chance one finds, it comes to (approximately) 0.56. This suggests there is some similarity between Y and Y', but this is misleading as we know any similarity is stochastic. In the same scenario the adjusted Rand index between the partitions is 0. This seems preferable. Based on this, one could argue that the Rand index has inflated values. Consider the case that we have n points in total, but we let the first $\frac{7n}{16}$ have a common label (say $(c_1, \ldots, c_{n_1}) = 1$ for $n_1 = \frac{7n}{16}$) and then draw the remaining $\frac{9n}{16}$ points from $\mathcal{U}\{1,3\}$. Then, as n tends to infinity, our contingency table tends to that described in table 2. One feels that the high Rand index for such a clustering, 0.64, is misleading in its magnitude. In such a scenario we feel one has to consider this 0.64 in the context of the 0.56 for a purely random similarity - this is difficult to do without explicitly checking what the Rand index is for a random partitioning for a given K and K'. Thus the use of the full unit interval in comparing similarity by a corrected index such as the adjusted Rand index requires less vigilance on the part of the analyst. In the second scenario, the adjusted Rand index is 0.28.

2.6 Standardisation

For a p-vector of observations, $X_i = (x_{i1}, \ldots, x_{1p})$, we define *standardisation* of X_i as the mapping from X_i to $X'_i = (x'_{i1}, \ldots, x'_{ip})$ defined by the *sample mean*, $\bar{x}_i$, and *sample standard deviation*, s_i:

$$\bar{x}_i = \frac{1}{p} \sum_{j=1}^{p} x_{ij} \tag{18}$$

$$s_i^2 = \frac{1}{p-1} \sum_{j=1}^{p} \left(x_{ij} - \bar{x}_i \right)^2 \tag{19}$$

$$x'_{ij} = \frac{x_{ij} - \bar{x}_i}{s_i} \quad \forall \quad j \in (1, \ldots, p) \tag{20}$$

6

We refer to X_i' as the standardised form of X. If we are given a dataset $X = (X_1, \ldots, X_n)$ where each X_i is a p-vector of observations of the form referred to above, then in referring to the standardised form of X, we mean the dataset $X' = (X_1', \ldots, X_n')$ where each X_i' is the standardised form of X_i.

Standardisation moves the values observed for each X_i to a common scale where each vector has an observed mean and standard deviation of 0 and 1 respectively.

We describe an example in section 2.9.1 which shows an explicit application and motivation for standardisation in the context of this project.

2.7 Consensus clustering

In the scenario that MDI struggles to explore the entire posterior distribution from any given initialisation for any realistic number of iterations of MCMC, we propose use of a "consensus" clustering [14]. In this scenario we draw samples of clusterings from MCMC chains with different initialisations and use these clusterings to describe the posterior distribution. In practice this involves running n_{seeds} different chains of MDI for a smaller number of iterations (some $n_{iter} \in [500, 1000]$), burning out the first $n_{iter} - 1$ iterations and saving the clustering from the final iteration. We then combine the clusterings from all n_{seeds} within a posterior similarity matrix (PSM), a $N \times N$ matrix where the (i, j) entry is the proportion of times genes i and j are in the same cluster. This means that the PSM is not affected by label-flipping and that it is a symmetric matrix with 1's along the diagonal and all entries in the unit interval. From this PSM a summary clustering may be calculated. The combination of different initialisations explores all the possible likelihood maixma and thus provides a more informed clustering. As the algorithm is not exploring the full space in any given iteration, we expect that the uncertainty quantification is optimistic, however we argue that an estimate made using insufficient data is better than one made using none at all and that this method is the best currently available to us for quantifying the uncertainty and exploring the posterior distribution.

2.8 Tissue specificity

Cell-type specific gene pathways are pivotal in differentiating tissue function, implicated in hereditary organ failure, and mediate acquired chronic disease [6]. More and more evidence is being accrued to highlight the cell-type specific level of gene expression [3][17][12].

We also see that there are many auto-immune disease, normally associated with a specific tissue type, that have strong genetic associations. Tissue specific isoforms and expression have also been observed [25]. This shows that genes have context-specific interactions that should be considered in analysis.

2.9 Gene sets

With the onset of microarrays and RNAseq, producing gene expression data in large quantities for a wide number of genes is increasingly enabled. Unfortunately the large amount of data gifted onto the genomics community by these methods is difficult to interpret and analyse. Gene Set Enrichment Analysis (GSEA) attempts to overcome some of these issues by analysing pre-defined gene sets and changes in the expression of the full set rather than considering each constituent member on an individual basis [15]. Consider, that in analysing gene sets as a group, the degree of perturbation in the expression of the full gene set due to the disease state / alternative phenotype that is required to be considered significant is much less than that required in analysing each of its constituent members individually [2][26]. This use of gene sets can increase the power of the analysis.

Furthermore, we know from Genome Wide Association Studies (GWAS) that many diseases are polygenic in nature [15]. Furthermore, Subramanian et al. [20] highlight the importance of gene sets, claiming that within a single metabolic pathway an increase of 20% in all the associated gene products may be more important than a 20-fold increase in a single gene.

Thus clustering genes into groups known as "gene sets" is natural and useful from both a biological and statistical perspective - it can increase the interpretability and the power of an analysis [16][24].

However, the problem of defining gene sets is non-trivial with many variations in-use. There exist many databases of gene sets [1][7][21]. The Molecular Signature Database [20] (MSigDB) is one of the most popular resources for GSEA and encompasses many different gene sets defined under various criteria or generated from separate resources. However, none of these definitions of a "set" incorporate tissue specific information. We believe that this is an oversight as there is evidence that some genes are involved in tissue specific pathways (see section 2.8). Thus we propose defining tissue specific gene sets. Previous attempts to achieve this have used the Genotype Tissue Expression (GTEx) [4] database [10], but here the profiles are for human donors post-mortem. We suspect that the data derived from these cells may not contain the same information as that collected from living, active cells. Furthermore, the GTEx data is across many different tissues (144 are used in [10]), but we focus on cell types relevant to autoimmune disease in general (i.e. blood cells) and IBD in particular (intestinal samples). This restricted focus should offer relevant gene sets.

Gene sets should contain sets of genes that have correlated expression. If this is the case, it is often assumed that the genes are common members of some metabolic pathway and that their products interact. As this correlated expression is represented by a common variation across people rather than in the magnitude of expression, we will standardise the expression data. We describe a small example to explain our reasoning.

8

Genes	Person 1	Person 2	Person 3	Person 4
A	5.1	5.2	4.9	5.0
B	5.1	4.9	5.2	5.4
C	1.4	1.5	1.2	1.3
D	1.4	1.2	1.5	1.7
E	1.4	1.5	1.4	1.5

Table 3: Example gene expression data.

2.9.1 Motivating example: Standardising gene expression data

If one considers table 3 which contains an example of expression data for some genes A, B, C, D and E across people 1 to 4. One can see that genes A and C have similar
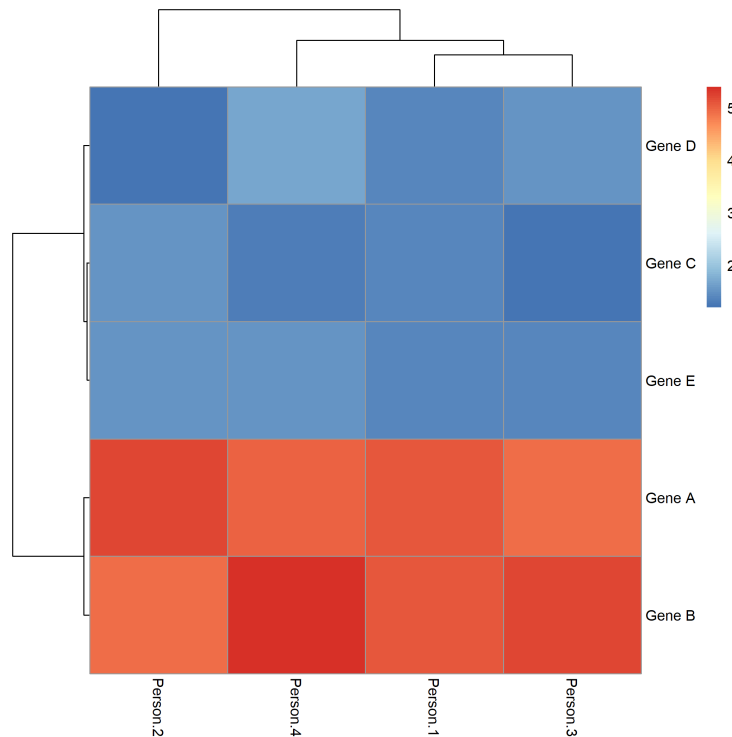
Figure 1: Heatmap of expression data in table 3 showing the clusters based upon magnitude of expression.

patters in variation across the people, as do genes B and D. Gene E is not consistent with any other gene here. However, as this relative variation is of interest rather than the magnitude of expression, one can see that standardising the data is required. If one were to cluster the data as represented in table 3, one would place genes A and B in one cluster and genes C, D and E in another as their absolute expression levels are similar (as can be seen in figure 1). However, if the expression level of each gene

9

Genes	Person 1	Person 2	Person 3	Person 4
A	0.39	1.16	-1.16	-0.39
B	-0.24	-1.20	0.24	1.20
C	0.39	1.16	-1.16	-0.39
D	-0.24	-1.20	0.24	1.20
E	-0.87	0.87	-0.87	0.87

Table 4: Example standardised gene expression data.

is standardised as per section 2.6, the data is then as represented in table 4. As the data are now on the same scale the characteristic that will determine a clustering is the variation of expression across people. As we want genes with similar patterns of variation (i.e. that are co-expressed) this enables us to cluster under our objective of defining gene sets. In this case genes A and C are one cluster, genes B and D another with gene E in a cluster alone, as can be seen in figure 2. As this is the type of data we wish to cluster across, we therefore most standardise our expression data before clustering can be implemented.
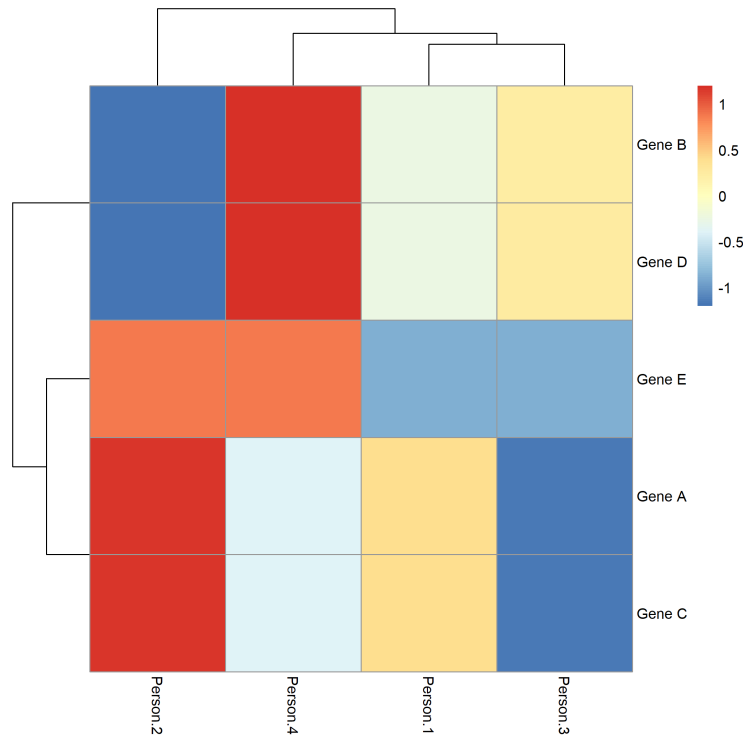
Figure 2: Heatmap of expression data in table 4 showing the clusters based upon variation of expression across people.

3 Data

The data is from the Correlated Expression and Disease Association Research (CEDAR) cohort [23]. We have 9 .csv files, one for each tissue / cell type present of normalised gene expression data for 323 individuals. These are healthy individuals of European descent; the cohort consists of 182 women and 141 men with an average age of 56 years (but ranging from 19 to 86). None of the individuals are suffering from any autoimmune or inflammatory disease and were not taking corticosteroids or non-steroid anti-inflammatory drugs (with the exception of aspirin).

With regards to tissue types, samples from six circulating immune cells types (followed in brackets by the abbreviation for the associated dataset):

- CD4+ T lymphocytes (CD4);
- CD8+ T lymphocytes (CD8);
- CD14+ monocytes (CD14);
- CD15+ granulocytes (CD15);
- CD19+ B lymphocytes (CD19); and
- platelets (PLA).

Data from intestinal biopsies are also present, with sample taken from three distinct locations:

- the illeum (IL);
- the rectum (RE); and
- the colon (TR).

Not every individual is present in every dataset. However, as we are clustering genes this should not present a problem.

Whole genome expression data were generated using HT-12 Expression Bead-chips following the instructions of the manufacturer (Illumina). $29,464$ autosomal probes (corresponding to 19,731 genes) were included across the datasets, but further thinning under various criteria reduced this further in each dataset. The final space of has 18,524 probes present between the 9 datsets.

The fluorescence intensities were $\log_2$ transformed and Robust Spline Normalized with Lumi38.

It should be noted that some datasets are less information rich than others (for instance the platelets dataset has 6,564 probes present in comparison to an average of 12,838 probes present per dataset, see figure 3). Due to this and the exponential increase in computational cost for each additional dataset, we use only the 8 most informative datasets, dropping PLA from our analysis. From a biological perspective we also expect PLA to be the least rich as platelets have no nucleus citeWRIGHT and therefore any gene expression is an artefact from before they differentiated into platelets.
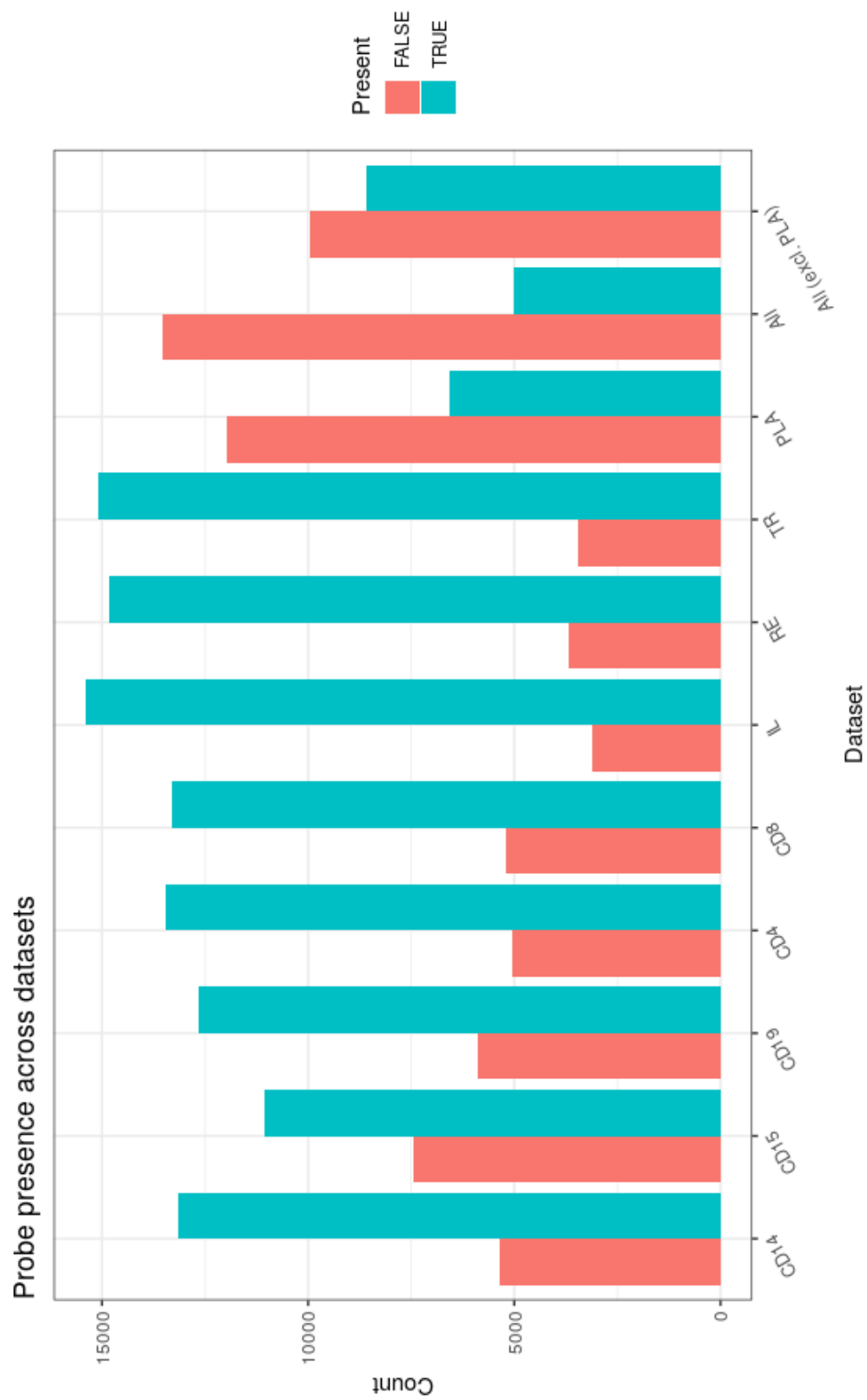
Figure 3: Probe presence across datasets. Under "All" we have the number of probes present in every dataset, under "All (excl. PLA)" we have the number of probes present in every dataset bar PLA. Note how PLA is less information rich than any other dataset.

4 Methods

We first show via simulated data that MDI can cluster appropriately and that the consensus clustering does produce similar results to a converged single run.

  We then simulate data where individual chains of MDI will struggle to converge and possibly will not converge in finite time. We show that consensus clustering explores a wider space than any individual chain and appears to describe something similar to the space described by the union of the chains.

  Finally we apply consensus clustering to 1,000 probes for 8 datasets from the CEDAR dataset. An initial set of probes are chosen based on the members of 3 KEGG pathways:

1. Inositol phosphate metabolism (a broad biological pathway);

2. NOD-like receptor signaling pathway (a specific biological pathway with known involvement in IBD citeCERNEIRO citeGARRETT); and

3. Inflammatory bowel disease (IBD) (a pathological pathway).

The union of these sets corresponds to 169 unique genes (or 287 probes as the mapping from the space of probes to that of genes is non-injective) that are present in the CEDAR dataset. The remaining probes are randomly selected from the total possible space (18,524 probes) less those corresponding to these genes (leaving 18,287 possible candidate probes). We then expect that the genes from the sets mentioned above (list 4) should cluster together. We use this as a test of our final clustering.

4.1 CEDAR data pipeline

For the CEDAR data, we follow this pipeline to prepare the data for clustering:

1. Transpose the data to have rows associated with gene probes and columns associated with individuals;

2. Remove NAs either imputing values using the minimum expressed value (as missingness is not random) or if above a threshold of missingness removing the column;

3. Standardise the data;

4. To apply MDI we require that each dataset have the same row names in the same order, so we re-arrange our datasets to have common order of probes;

5. For probes entirely missing from a given dataset we generate expression from a standard normal distribution for each probe. Then these probes are expressed as noise in the dataset and any clustering imposed upon them should be due to information about these probes present in other datasets; and

6. Apply MDI [13].

13

5 Results

5.1 Case 1: Proof of consensus

Generated data based on data from original MDI paper with some additional noisy clusters that MDI succeeds with.

5.2 Case 2: Overcoming multiple modes

Generated data that MDI struggles with.
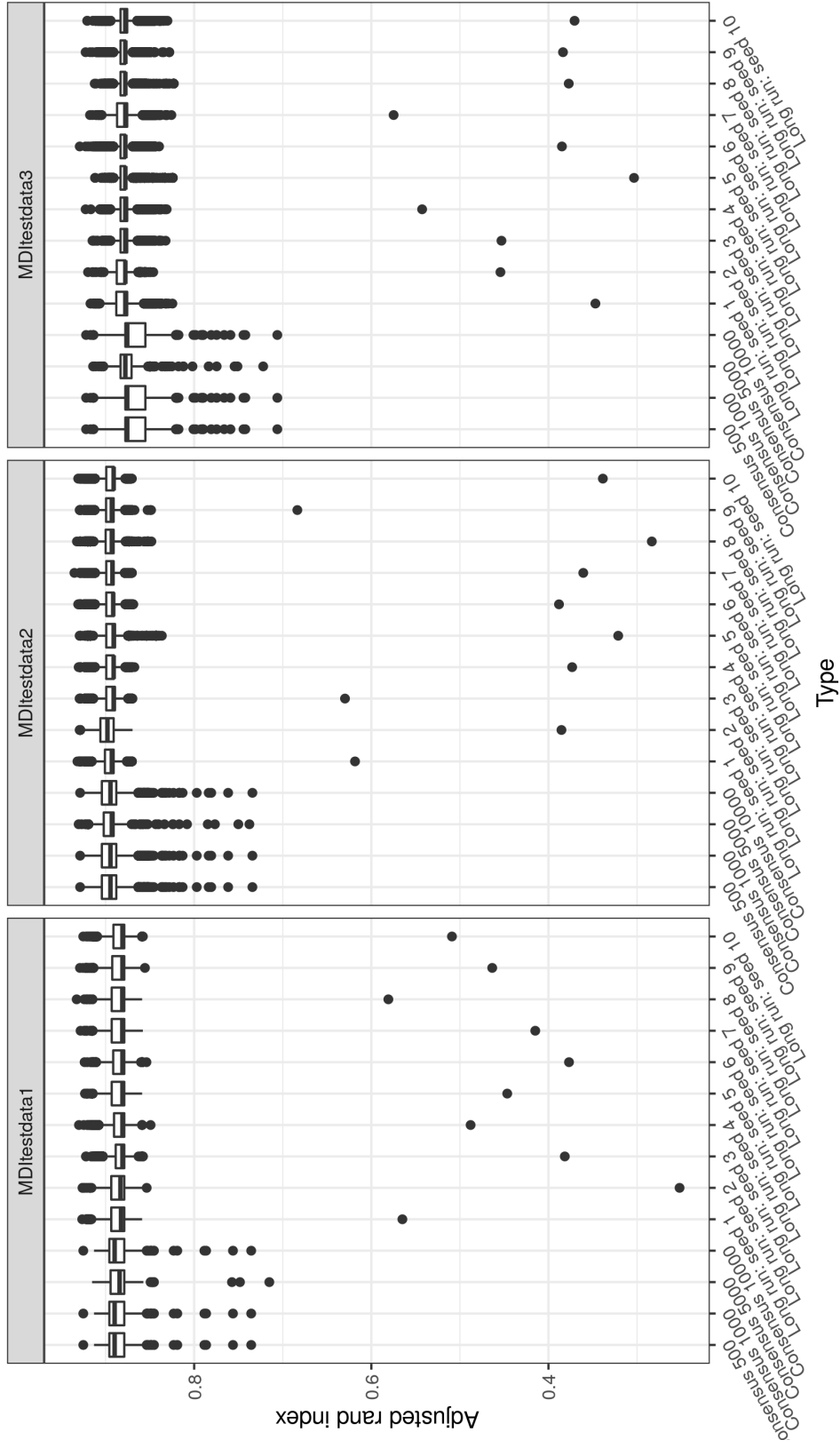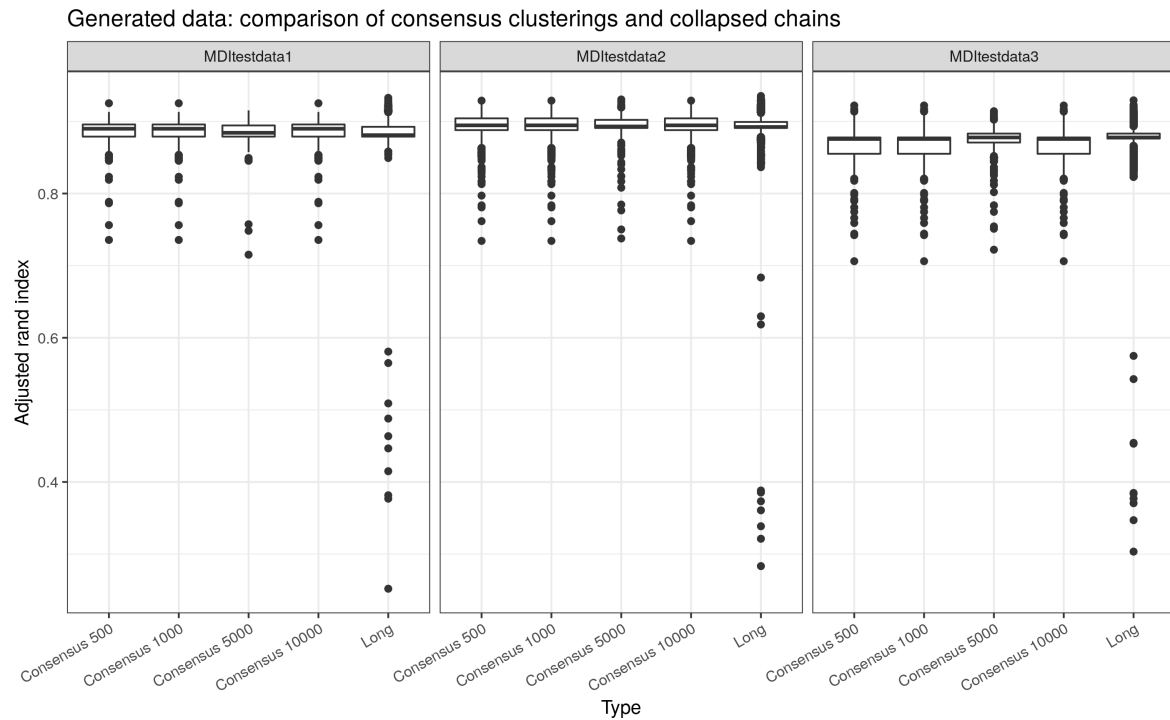
5.3 Case 3: CEDAR data

Actual data.

Figure 4: Box plots for distribution of adjusted rand index between the clustering at each iteration to the true clustering for different lengths of consensus clustering and different initialisation of long chains.

Generated data: comparison of consensus clusterings and collapsed chains

Figure 5: Box plots for distribution of adjusted rand index between the clustering at each iteration to the true clustering for different lengths of consensus clustering and the collapsed long chains.

References

[1] Michael Ashburner, Catherine A. Ball, Judith A. Blake, David Botstein, Heather Butler, J. Michael Cherry, Allan P. Davis, Kara Dolinski, Selina S. Dwight, Janan T. Eppig, Midori A. Harris, David P. Hill, Laurie Issel-Tarver, Andrew Kasarskis, Suzanna Lewis, John C. Matese, Joel E. Richardson, Martin Ringwald, Gerald M. Rubin, and Gavin Sherlock. Gene Ontology: Tool for the unification of biology. *Nature Genetics*, 25(1):25–29, May 2000. ISSN 1061-4036, 1546-1718. doi: 10.1038/75556.

[2] Frank Dudbridge. Power and Predictive Accuracy of Polygenic Risk Scores. *PLoS Genetics*, 9(3):e1003348, March 2013. ISSN 1553-7404. doi: 10.1371/journal. pgen.1003348.

[3] Elin Grundberg, Kerrin S Small, Åsa K Hedman, Alexandra C Nica, Alfonso Buil, Sarah Keildson, Jordana T Bell, Tsun-Po Yang, Eshwar Meduri, Amy Barrett, James Nisbett, Magdalena Sekowska, Alicja Wilk, So-Youn Shin, Daniel Glass, Mary Travers, Josine L Min, Sue Ring, Karen Ho, Gudmar Thorleifsson, Augustine Kong, Unnur Thorsteindottir, Chrysanthi Ainali, Antigone S
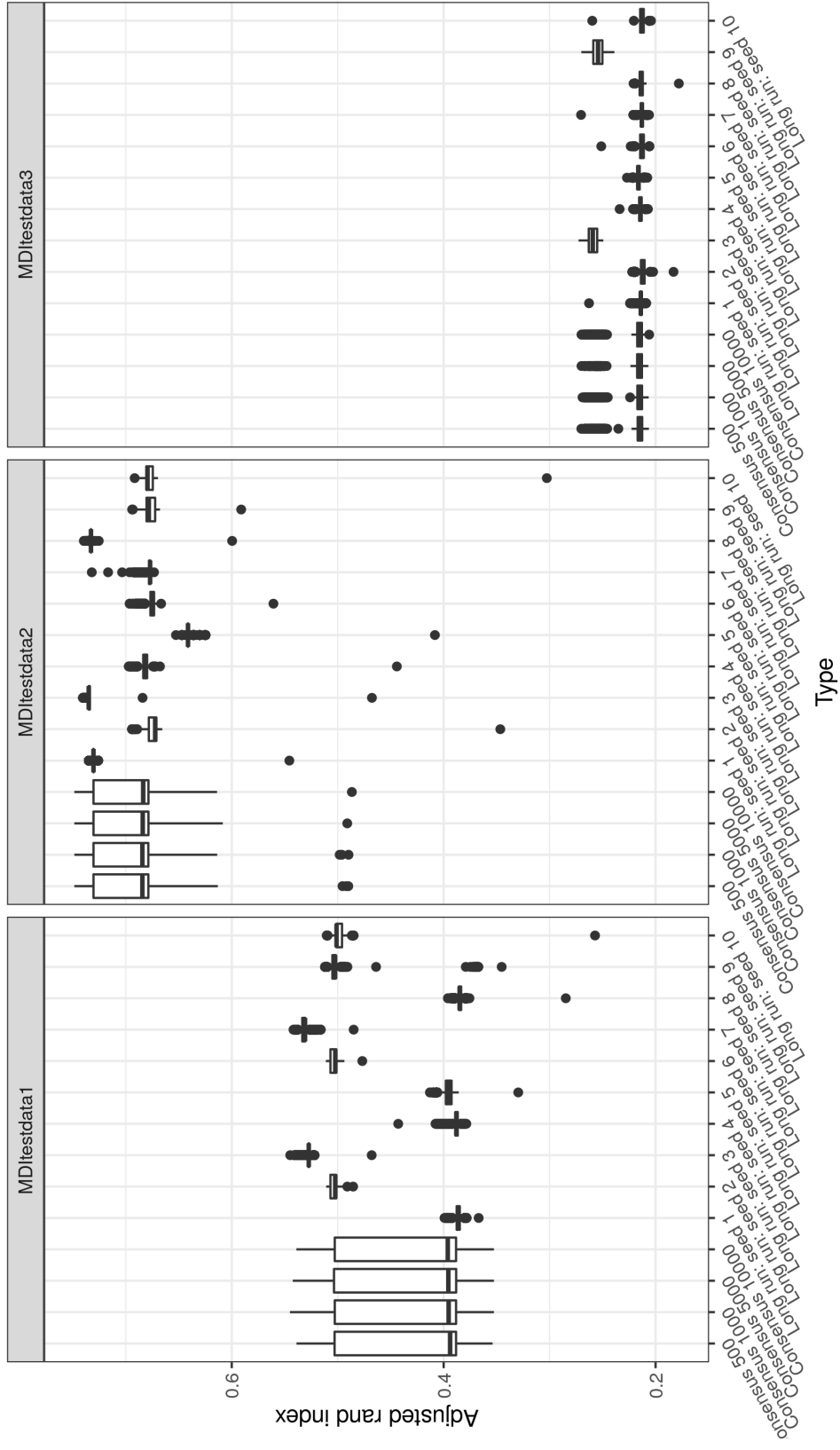
16

Figure 6: Box plots for distribution of adjusted rand index between the clustering at each iteration to the true clustering for different lengths of consensus clustering and different initialisation of long chains.
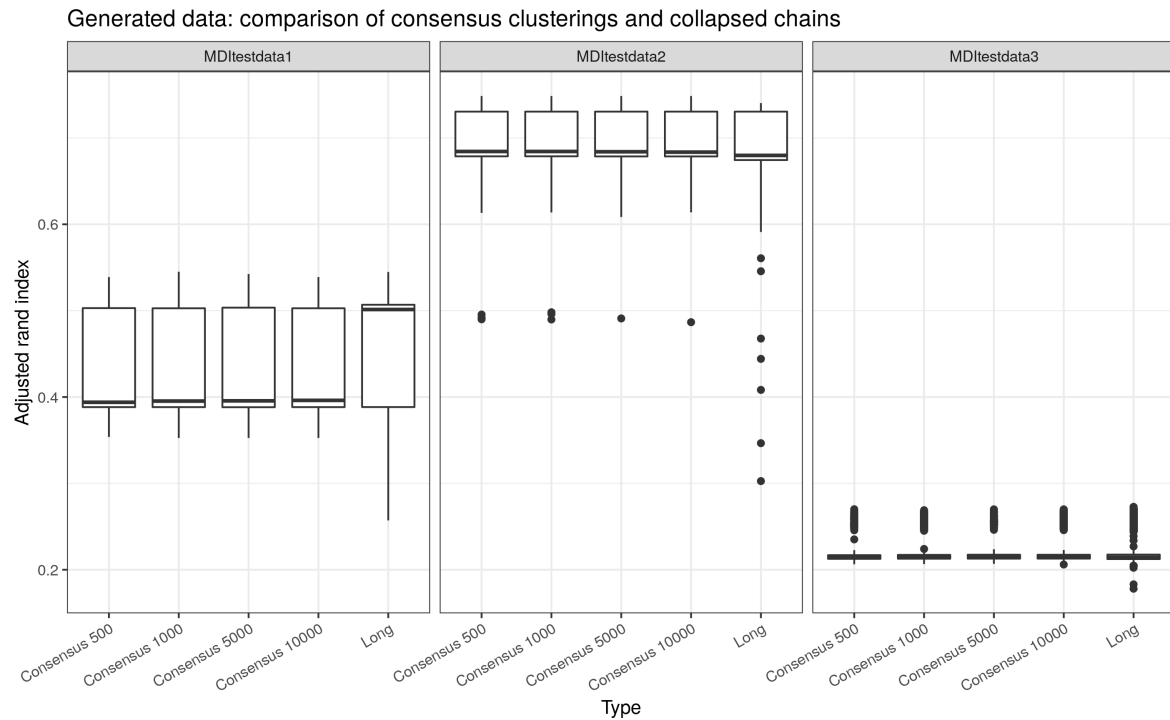
Figure 7: Box plots for distribution of adjusted rand index between the clustering at each iteration to the true clustering for different lengths of consensus clustering and the collapsed long chains.

Dimas, Neelam Hassanali, Catherine Ingle, David Knowles, Maria Krestyaninova, Christopher E Lowe, Paola Di Meglio, Stephen B Montgomery, Leopold Parts, Simon Potter, Gabriela Surdulescu, Loukia Tsaprouni, Sophia Tsoka, Veronique Bataille, Richard Durbin, Frank O Nestle, Stephen O'Rahilly, Nicole Soranzo, Cecilia M Lindgren, Krina T Zondervan, Kourosh R Ahmadi, Eric E Schadt, Kari Stefansson, George Davey Smith, Mark I McCarthy, Panos Deloukas, Emmanouil T Dermitzakis, and Tim D Spector. Mapping cis- and trans-regulatory effects across multiple tissues in twins. *Nature Genetics*, 44(10):1084–1089, October 2012. ISSN 1061-4036, 1546-1718. doi: 10.1038/ng.2394.

[4] GTEx Consortium. Genetic effects on gene expression across human tissues. *Nature*, 550(7675):204–213, October 2017. ISSN 0028-0836, 1476-4687. doi: 10.1038/nature24277.

[5] Lawrence Hubert and Phipps Arabie. Comparing partitions. *Journal of Classification*, 2(1):193–218, December 1985. ISSN 0176-4268, 1432-1343. doi: 10.1007/BF01908075.

[6] Wenjun Ju, Casey S. Greene, Felix Eichinger, Viji Nair, Jeffrey B. Hodgin, Markus Bitzer, Young-suk Lee, Qian Zhu, Masami Kehata, Min Li, Song Jiang,
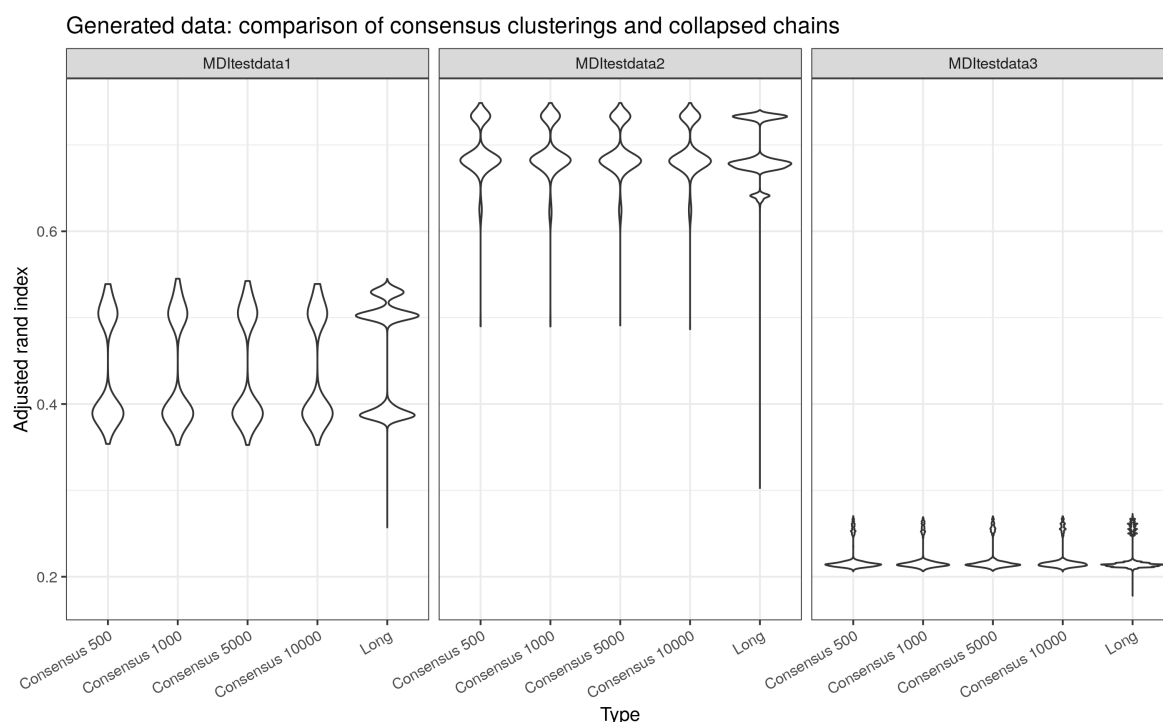
Figure 8: Violoin plots for distribution of adjusted rand index between the clustering at each iteration to the true clustering for different lengths of consensus clustering and the collapsed long chains. We can see that the consensus clustering approximates the modes described across chains quite well.

Maria Pia Rastaldi, Clemens D. Cohen, Olga G. Troyanskaya, and Matthias Kretzler. Defining cell-type specificity at the transcriptional level in human disease. *Genome Research*, 23(11):1862–1873, November 2013. ISSN 1088-9051. doi: 10.1101/gr.155697.113.

[7] Minoru Kanehisa, Yoko Sato, Miho Furumichi, Kanae Morishima, and Mao Tanabe. New approach for understanding genome variations in KEGG. *Nucleic Acids Research*, 47(D1):D590–D595, January 2019. ISSN 0305-1048, 1362-4962. doi: 10.1093/nar/gky962.

[8] Paul Kirk, Jim E. Griffin, Richard S. Savage, Zoubin Ghahramani, and David L. Wild. Bayesian correlated clustering to integrate multiple datasets. *Bioinformatics*, 28(24):3290–3297, December 2012. ISSN 1460-2059, 1367-4803. doi: 10.1093/bioinformatics/bts595.

[9] Raivo Kolde. Pheatmap: Pretty Heatmaps, 2018. R package version 1.0.10.

[10] John Lonsdale, Jeffrey Thomas, Mike Salvatore, Rebecca Phillips, Edmund Lo, Saboor Shad, Richard Hasz, Gary Walters, Fernando Garcia, Nancy Young,

Barbara Foster, Mike Moser, Ellen Karasik, Bryan Gillard, Kimberley Ramsey, Susan Sullivan, Jason Bridge, Harold Magazine, John Syron, Johnelle Fleming, Laura Siminoff, Heather Traino, Maghboeba Mosavel, Laura Barker, Scott Jewell, Dan Rohrer, Dan Maxim, Dana Filkins, Philip Harbach, Eddie Cortadillo, Bree Berghuis, Lisa Turner, Eric Hudson, Kristin Feenstra, Leslie Sobin, James Robb, Phillip Branton, Greg Korzeniewski, Charles Shive, David Tabor, Liqun Qi, Kevin Groch, Sreenath Nampally, Steve Buia, Angela Zimmerman, Anna Smith, Robin Burges, Karna Robinson, Kim Valentino, Deborah Bradbury, Mark Cosentino, Norma Diaz-Mayoral, Mary Kennedy, Theresa Engel, Penelope Williams, Kenyon Erickson, Kristin Ardlie, Wendy Winckler, Gad Getz, David DeLuca, Daniel MacArthur, Manolis Kellis, Alexander Thomson, Taylor Young, Ellen Gelfand, Molly Donovan, Yan Meng, George Grant, Deborah Mash, Yvonne Marcus, Margaret Basile, Jun Liu, Jun Zhu, Zhidong Tu, Nancy J Cox, Dan L Nicolae, Eric R Gamazon, Hae Kyung Im, Anuar Konkashbaev, Jonathan Pritchard, Matthew Stevens, Timothèe Flutre, Xiaoquan Wen, Emmanouil T Dermitzakis, Tuuli Lappalainen, Roderic Guigo, Jean Monlong, Michael Sammeth, Daphne Koller, Alexis Battle, Sara Mostafavi, Mark McCarthy, Manual Rivas, Julian Maller, Ivan Rusyn, Andrew Nobel, Fred Wright, Andrey Shabalin, Mike Feolo, Nataliya Sharopova, Anne Sturcke, Justin Paschal, James M Anderson, Elizabeth L Wilder, Leslie K Derr, Eric D Green, Jeffery P Struewing, Gary Temple, Simona Volpi, Joy T Boyer, Elizabeth J Thomson, Mark S Guyer, Cathy Ng, Assya Abdallah, Deborah Colantuoni, Thomas R Insel, Susan E Koester, A Roger Little, Patrick K Bender, Thomas Lehner, Yin Yao, Carolyn C Compton, Jimmie B Vaught, Sherilyn Sawyer, Nicole C Lockhart, Joanne Demchok, and Helen F Moore. The Genotype-Tissue Expression (GTEx) project. *Nature Genetics*, 45(6):580–585, June 2013. ISSN 1061-4036, 1546-1718. doi: 10.1038/ng.2653.

[11] David J C MacKay. *Information Theory, Inference, and Learning Algorithms*. September 2003.

[12] T Maniatis, S Goodbourn, and J. Fischer. Regulation of inducible and tissue-specific gene expression. *Science*, 236(4806):1237–1245, June 1987. ISSN 0036-8075, 1095-9203. doi: 10.1126/science.3296191.

[13] Samuel A. Mason, Faiz Sayyid, Paul D.W. Kirk, Colin Starr, and David L. Wild. MDI-GPU: Accelerating integrative modelling for genomic-scale data using GP-GPU computing. *Statistical Applications in Genetics and Molecular Biology*, 15 (1), January 2016. ISSN 1544-6115, 2194-6302. doi: 10.1515/sagmb-2015-0055.

[14] Stefano Monti. Consensus Clustering: A Resampling-Based Method for Class Discovery and Visualization of Gene Expression Microarray Data. page 28.

[15] Michael A. Mooney and Beth Wilmot. Gene set analysis: A step-by-step guide.

American Journal of Medical Genetics Part B: Neuropsychiatric Genetics, 168(7):517–527, October 2015. ISSN 15524841. doi: 10.1002/ajmg.b.32328.

[16] A. C. Nica and E. T. Dermitzakis. Expression quantitative trait loci: Present and future. *Philosophical Transactions of the Royal Society B: Biological Sciences*, 368(1620):20120362–20120362, May 2013. ISSN 0962-8436, 1471-2970. doi: 10.1098/rstb.2012.0362.

[17] Chin-Tong Ong and Victor G. Corces. Enhancer function: New insights into the regulation of tissue-specific gene expression. *Nature Reviews Genetics*, 12(4): 283–293, April 2011. ISSN 1471-0056, 1471-0064. doi: 10.1038/nrg2957.

[18] William N. Rand. Objective Criteria for the Evaluation of Clustering Methods. *Journal of the American Statistical association*, 66(336):846–850, 1971.

[19] Richard S. Savage, Zoubin Ghahramani, Jim E. Griffin, Paul Kirk, and David L. Wild. Identifying cancer subtypes in glioblastoma by combining genomic, transcriptomic and epigenomic data. *arXiv:1304.3577 [q-bio, stat]*, April 2013.

[20] A. Subramanian, P. Tamayo, V. K. Mootha, S. Mukherjee, B. L. Ebert, M. A. Gillette, A. Paulovich, S. L. Pomeroy, T. R. Golub, E. S. Lander, and J. P. Mesirov. Gene set enrichment analysis: A knowledge-based approach for interpreting genome-wide expression profiles. *Proceedings of the National Academy of Sciences*, 102(43):15545–15550, October 2005. ISSN 0027-8424, 1091-6490. doi: 10.1073/pnas.0506580102.

[21] Damian Szklarczyk, Annika L Gable, David Lyon, Alexander Junge, Stefan Wyder, Jaime Huerta-Cepas, Milan Simonovic, Nadezhda T Doncheva, John H Morris, Peer Bork, Lars J Jensen, and Christian von Mering. STRING v11: Protein–protein association networks with increased coverage, supporting functional discovery in genome-wide experimental datasets. *Nucleic Acids Research*, 47(D1):D607–D613, January 2019. ISSN 0305-1048, 1362-4962. doi: 10.1093/nar/gky1131.

[22] R Core Team. R: A Language and Environment for Statistical Computing. R Foundation for Statistical Computing, 2018.

[23] The International IBD Genetics Consortium, Yukihide Momozawa, Julia Dmitrieva, Emilie Théâtre, Valérie Deffontaine, Souad Rahmouni, Benoît Charloteaux, François Crins, Elisa Docampo, Mahmoud Elansary, Ann-Stephan Gori, Christelle Lecut, Rob Mariman, Myriam Mni, Cécile Oury, Ilya Altukhov, Dmitry Alexeev, Yuri Aulchenko, Leila Amininejad, Gerd Bouma, Frank Hoentjen, Mark Löwenberg, Bas Oldenburg, Marieke J. Pierik, Andrea E. vander Meulen-de Jong, C. Janneke van der Woude, Marijn C. Visschedijk, Mark Lathrop, Jean-Pierre Hugot, Rinse K. Weersma, Martine De Vos, Denis Franchimont,

Severine Vermeire, Michiaki Kubo, Edouard Louis, and Michel Georges. IBD risk loci are enriched in multigenic regulatory modules encompassing putative causative genes. *Nature Communications*, 9(1):2427, December 2018. ISSN 2041-1723. doi: 10.1038/s41467-018-04365-8.

[24] Urmo Võsa, Annique Claringbould, Harm-Jan Westra, Marc Jan Bonder, Patrick Deelen, Biao Zeng, Holger Kirsten, Ashis Saha, Roman Kreuzhuber, Silva Kasela, Natalia Pervjakova, Isabel Alvaes, Marie-Julie Fave, Mawusse Agbessi, Mark Christiansen, Rick Jansen, Ilkka Seppälä, Lin Tong, Alexander Teumer, Katharina Schramm, Gibran Hemani, Joost Verlouw, Hanieh Yaghootkar, Reyhan Sönmez, Andrew A. Andrew, Viktorija Kukushkina, Anette Kalnapenkis, Sina Rüeger, Eleonora Porcu, Jaanika Kronberg-Guzman, Johannes Kettunen, Joseph Powell, Bernett Lee, Futao Zhang, Wibowo Arindrarto, Frank Beutner, BIOS Consortium, Harm Brugge, i2QTL Consortium, Julia Dmitrieva, Mahmoud Elansary, Benjamin P. Fairfax, Michel Georges, Bastiaan T Heijmans, Mika Kähönen, Yungil Kim, Julian C. Knight, Peter Kovacs, Knut Krohn, Shuang Li, Markus Loeffler, Urko M Marigorta, Hailang Mei, Yukihide Momozawa, Martina Müller-Nurasyid, Matthias Nauck, Michel Nivard, Brenda Penninx, Jonathan Pritchard, Olli Raitakari, Olaf Rotzschke, Eline P. Slagboom, Coen D.A. Stehouwer, Michael Stumvoll, Patrick Sullivan, Peter A.C. 't Hoen, Joachim Thiery, Anke Tönjes, Jenny van Dongen, Maarten van Iterson, Jan Veldink, Uwe Völker, Cisca Wijmenga, Morris Swertz, Anand Andiappan, Grant W. Montgomery, Samuli Ripatti, Markus Perola, Zoltan Kutalik, Emmanouil Dermitzakis, Sven Bergmann, Timothy Frayling, Joyce van Meurs, Holger Prokisch, Habibul Ahsan, Brandon Pierce, Terho Lehtimäki, Dorret Boomsma, Bruce M. Psaty, Sina A. Gharib, Philip Awadalla, Lili Milani, Willem H. Ouwehand, Kate Downes, Oliver Stegle, Alexis Battle, Jian Yang, Peter M. Visscher, Markus Scholz, Gregory Gibson, Tõnu Esko, and Lude Franke. Unraveling the polygenic architecture of complex traits using blood eQTL meta-analysis. Preprint, Genomics, October 2018.

[25] Eric T. Wang, Rickard Sandberg, Shujun Luo, Irina Khrebtukova, Lu Zhang, Christine Mayr, Stephen F. Kingsmore, Gary P. Schroth, and Christopher B. Burge. Alternative isoform regulation in human tissue transcriptomes. *Nature*, 456(7221):470–476, November 2008. ISSN 0028-0836, 1476-4687. doi: 10.1038/nature07509.

[26] Naomi R. Wray, Sang Hong Lee, Divya Mehta, Anna A.E. Vinkhuyzen, Frank Dudbridge, and Christel M. Middeldorp. Research Review: Polygenic methods and their application to psychiatric traits. *Journal of Child Psychology and Psychiatry*, 55(10):1068–1087, October 2014. ISSN 00219630. doi: 10.1111/jcpp.12295.